Available online at www.sciencedirect.com

ScienceDirect

Ceramics International 35 (2009) 1243–1247

CERAMICS INTERNATIONAL

www.elsevier.com/locate/ceramint

Design of SiO_2/ZrO_2 core–shell particles using the sol–gel process

Jong Min Kim [a], Sang Mok Chang [a], Sungkook Kim [b], Kyo-Seon Kim [c], Jinsoo Kim [b], Woo-Sik Kim [b,*]

[a] Department of Chemical Engineering, Dong-A University, Busan 604-714, Republic of Korea
[b] Department of Chemical Engineering, Kyunghee University, Kyungki-do 446-701, Republic of Korea
[c] Department of Chemical Engineering, Kangwon National University, Kangwon-do 200-701, Republic of Korea

Received 3 April 2008; received in revised form 20 April 2008; accepted 16 June 2008
Available online 16 July 2008

Abstract

Core–shell particles of SiO_2/ZrO_2 were developed using a sol–gel process. Spherical core particles of SiO_2, 320 nm in diameter, were initially prepared using tetraethylorthosilicate (TEOS), and then uniformly shelled with ZrO_2 nano-particles synthesized with zirconium(IV) butoxide (TBOZ). The deposition of ZrO_2 nano-particles on the SiO_2 core particles was generally promoted when increasing the H_2O and TBOZ concentrations and temperature of the sol–gel process. However, micron-sized homo-aggregates of ZrO_2 were formed above certain concentrations of H_2O and TBOZ due to self-aggregation of the nano-ZrO_2 particles. It was very interesting to discover that a chemical bonding between zirconium and silicon bridged by oxygen (Si–O–Zr bond) was developed during the formation of the ZrO_2 shell around the core particles, as the silane groups on the core particles were condensed with zirconium hydroxyl groups during the deposition of ZrO_2. XPS and FT-IR confirmed the chemical bonding of Si–O–Zr in the core–shell particles.

Keywords: Core–shell particles; Sol–gel process; Nano-particles of ZrO_2; Chemical binding

1. Introduction

The design of composite particles has recently attracted a great deal of research attention due to the strong application potential of such particles in a variety of areas, including photocatalysts, white pigment, electronic devices, cosmetics, and fillers, etc. [1,2]. In particular, the unique ability of composites to compensate and reinforce material properties has resulted in extensive research efforts on controlling the design of core–shell particles [3,4].

Various approaches have been used to prepare core–shell particles, such as metal precursor reduction, thermal evaporation, electroless plating, and the sol–gel method. For example, Ocaña et al. [5] coated SiO_2 core particles with Fe metal using a metal precursor reaction. However, despite great care in the Fe metal deposition on the core particles under experimental conditions of aging and suspension agitation, complete coverage of the core particles by the Fe shell was rare and modification of the shell thickness was extremely limited, indicating the need for a surfactant additive for a uniform deposition of Fe metal on the core particle and an extra step of washing to obtain the pure core–shell particles. Meanwhile, Kobayashi et al. applied electroless plating to prepare core–shell particles of SiO_2–Ag [6], including pretreatment of the core particles with Sn ions to facilitate Ag deposition on the core particles. Nonetheless, the formation of a complete shell around the core particles was still hard to achieve. Among various studies on SiO_2–ZrO_2 materials, most of them focused on design of the composite particles of SiO_2 and ZrO_2 and the deposition of ZrO_2 on a flat surface of a SiO_2 substrate [7,8]. There has little been an attempt to the design of core–shell particles of SiO_2–ZrO_2 materials.

Accordingly, this study presents a method for creating uniform core–shell particles of SiO_2–ZrO_2 using a simple sol–gel process. In addition, the mechanism of ZrO_2 deposition on SiO_2 core particles is investigated using FT-IR and XPS, allowing the properties of the core–shell particles to be designed.

---

* Corresponding author. Tel.: +82 31 201 2576; fax: +82 31 273 2971.
E-mail address: wskim@khu.ac.kr (W.-S. Kim).

0272-8842/$34.00 © 2008 Elsevier Ltd and Techna Group S.r.l. All rights reserved.
doi:10.1016/j.ceramint.2008.06.003

2. Materials and methods

2.1. Preparation of SiO_2 core particles

Mono-dispersed spherical SiO_2 particles were prepared as core particles in a Rushton tank reactor using a sol–gel process. After initially loading a 330 ml mixture solution of ammonium hydroxide (ACS grade, Aldrich, U.S.A.) and methanol (ACS grade, Fluska, Switzerland), a 100 ml mixture solution of tetraethylorthosilicate (TEOS, ACS grade, Fluka, Switzerland) and methanol was fed into the reactor for 25 min, then the suspension was aged with agitation for 2 h to complete the sol–gel process [9]. The TEOS, ammonia, and H_2O concentrations used to prepare the silica core particles were always fixed at 0.48, 3.48, and 4.88 mol/l, respectively. The product suspension was filtered with ethanol washing, and then dried in an oven at 100 °C for 24 h. A typical particle size of around 320 nm with a high mono-dispersity was obtained for the core SiO_2 particles.

2.2. Zirconia coating on silica particles

To prepare the core–shell particles of SiO_2–ZrO_2, 1.0 g of the SiO_2 core particles was initially dispersed in a 60 ml mixture solution of ethanol and H_2O using an ultrasonicator in the Rushton tank reactor. A 40 ml mixture solution of zirconium(IV) butoxide (TBOZ, 80%, Aldrich, U.S.A.) and ethanol was then slowly injected into the reactor for 2 h, followed by aging for 2 h and heating under reflux at 80 °C for 90 min to complete the sol–gel process. Thereafter, the product suspension was filtered out and washed with pure ethanol. During the washing, the product samples were treated using an ultrasonic homogenizer (Model Cp505, Cole-Parmer, USA) to prevent any particle aggregation. Finally, the samples were dried in an oven at 100 °C for 24 h.

2.3. Analysis of particles

The shape, mono-dispersity, and size of the particles were all measured using FE-SEM (Model Leo-Supra 55, Carl Zeiss STM, Germany), while transmission electron microscopy (TEM, Model JEM-3000F, JEOL, Japan) at 300 kV was used to monitor the shell thickness of ZrO_2. An electrophoresis instrument (Model ELS-8000, Otsuka, Japan) was used to measure the zeta potentials of the particles, and their chemical bonds were examined using FT-IR (PerkinElmer, California, USA) and AES-XPS (Model ESCA-2000, VG Microtech, UK) with Mg Kα (1253.6 eV) radiation as the excitation source. The binding energies were calibrated relative to the C1s peak (284.8 eV) from the hydrocarbons absorbed on the surface of the samples.

3. Results and discussion

According to the sol–gel process, ZrO_2 was generated by the hydrolysis and condensation of TBOZ, and then deposed on SiO_2 core particles to form a shell layer, as shown in Fig. 1. The smooth surface of the SiO_2 core particles (Fig. 1(b)) was roughened on a nano-scale (Fig. 1(c)) due to the deposition of the nano-particles of ZrO_2, which were so unstable as to be easily attached to a foreign surface. Also, a uniform shell of

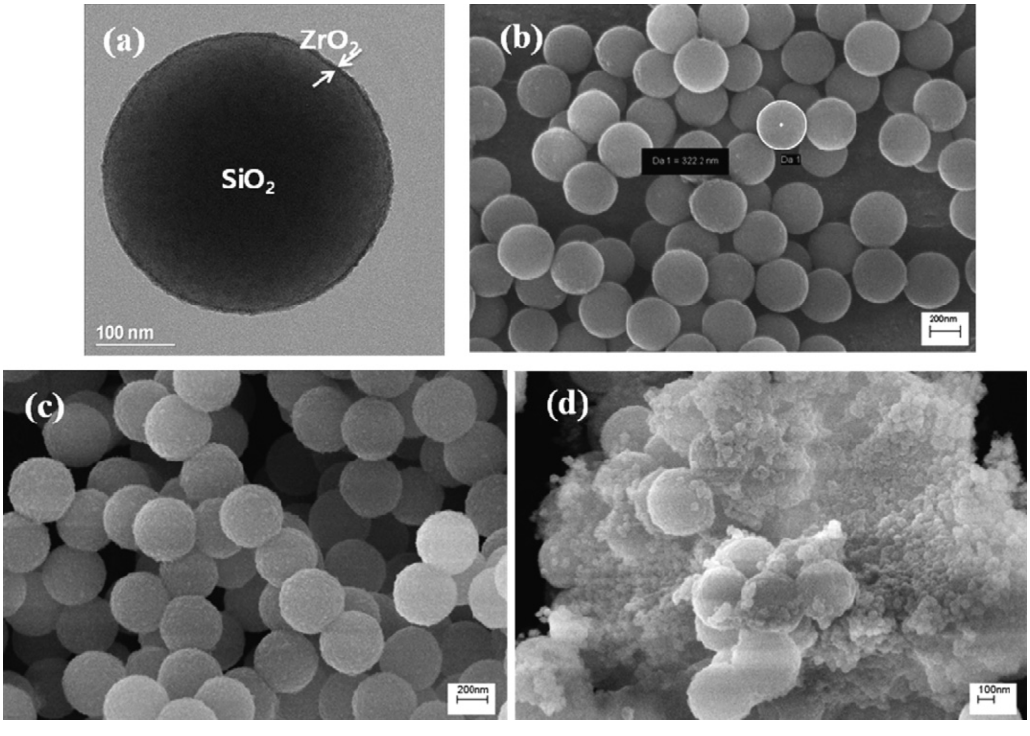

Fig. 1. Typical morphology of SiO_2–ZrO_2 core–shell particles prepared under various reaction conditions of sol–gel process: (a) TEM image of core–shell particles, (b) SEM image of SiO_2 core particles, (c) SEM image of core–shell particles prepared at 0.02 mol/l of TBOZ, and (d) SEM image of core–shell particles prepared at 0.14 mol/l of TBOZ. The other reaction conditions of H_2O and temperature were fixed at 0.56 mol/l and 40 °C, respectively.

ZrO_2 with a nano-scale thickness was confirmed by TEM images (Fig. 1(a)). The production of a uniform shape of core–shell particles was directly dictated by the ZrO_2 nano-particle generation and its deposition on the core particles. That is, when the generation rate of ZrO_2 nano-particles by the sol–gel process was below the deposition rate of ZrO_2 particles on the core particles, all the ZrO_2 particles were consumed to form the shell layer (Fig. 1(c)). However, when the ZrO_2 particle generation rate exceeded the ZrO_2 particle consumption rate by shell deposition, this resulted in the self-aggregation of ZrO_2 and stable homo-aggregates of ZrO_2, as shown in Fig. 1(d). Therefore, the experimental results strongly called for careful control of the generation rate of ZrO_2 nano-particles by adjusting the reaction conditions for the hydrolysis and condensation, including the TBOZ and H_2O concentrations and reaction temperature in the sol–gel process.

Since TBOZ was a reactant in the hydrolysis and condensation, the generation of ZrO_2 nano-particles was expected to be promoted when increasing the concentration of TBOZ, thereby thickening the shell layer. Thus, up to a TBOZ concentration of 0.065 mol/l, uniform core–shell particles were produced and the layer thickness of the core–shell particles increased up to 15 nm, as shown in Fig. 2. However, when increasing the TBOZ concentration beyond 0.065 mol/l, self-aggregation of the ZrO_2 particles occurred, resulting in homo-aggregates of ZrO_2, as the ZrO_2 generation exceeded the ZrO_2 consumption by deposition on the core particles. A similar shell-thickness dependency was also observed with the H_2O concentration, as shown in Fig. 3, where the shell thickness improved when increasing the H_2O up to 0.6 mol/l, as the deposition of ZrO_2 particles on the core particles was fast enough to consume the ZrO_2 particles generated by the reactions within this range of H_2O concentrations. However, beyond 0.6 mol/l of H_2O, the ZrO_2 particle generation became faster than the ZrO_2 particle deposition on the core particles, resulting in homo-aggregates of ZrO_2 particles in the product. It should also be noted that no shell layer of ZrO_2 was formed on the core particles without H_2O, as H_2O was the reactant for the hydrolysis of TBOZ.

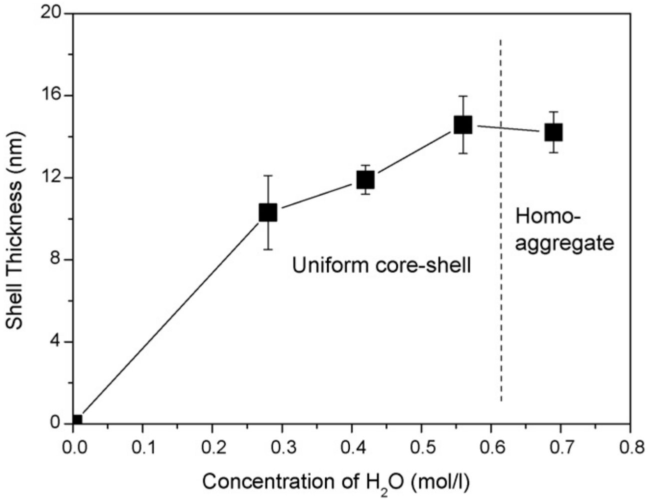

Fig. 3. Change of shell thickness of core–shell particles according to H_2O concentration. The TBOZ and temperature were fixed at 0.065 mol/l and 40 °C, respectively.

The influence of the reaction temperature on the ZrO_2 deposition and shell thickness was also measured, as shown in Fig. 4. The shell thickness of ZrO_2 was almost insensitive to the reaction temperature up to 60 °C, then suddenly decreased above 70 °C due to the self-aggregation of ZrO_2 particles. According to Iler [10], since temperature is known to accelerate ZrO_2 gelling, the generation of ZrO_2 particles is facilitated when increasing the temperature. Therefore, at a temperature range below 60 °C, it would seem that the deposition of ZrO_2 particles was high enough to consume the generated ZrO_2 particles, whereas above 70 °C, the generation of ZrO_2 particles exceeded the ZrO_2deposition on the core particles, resulting in homo-aggregates of ZrO_2 and a reduction of the shell thickness on the core particles. It should be noted that the hydrolysis and condensation of TBOZ were significantly depressed and

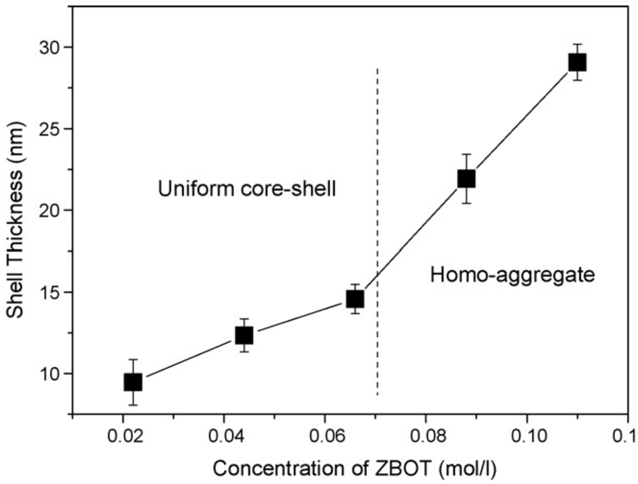

Fig. 2. Change of shell thickness of core–shell particles according to TBOZ concentration. The H_2O and temperature were fixed at 0.56 mol/l and 40 °C, respectively.

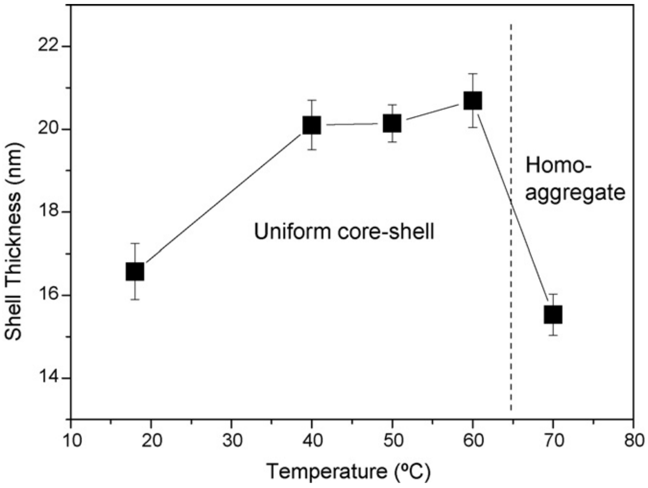

Fig. 4. Change of shell thickness of core–shell particles according to reaction temperature. The TBOZ and H_2O were fixed at 0.065 mol/l and 0.56 mol/l, respectively.

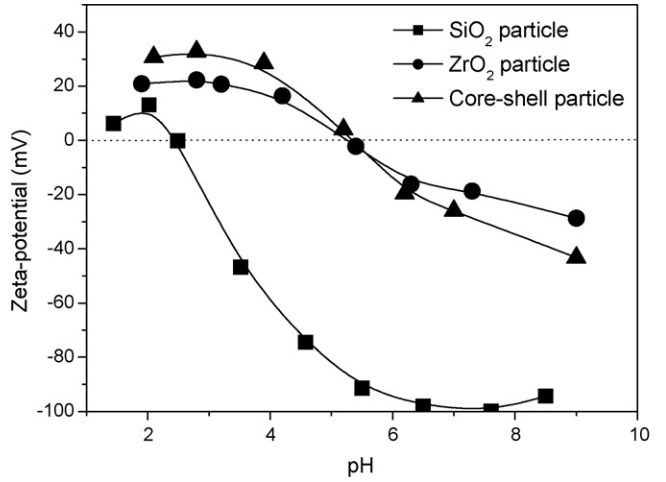

Fig. 5. Zeta-potential profiles of SiO_2, ZrO_2 and core–shell particles according to pH.

incomplete within the experiment time at a low reaction temperature of 18 °C, leading to a thin ZrO_2 shell.

The zeta-potential of the core–shell particles was measured to confirm the uniformity of the ZrO_2 shell around the SiO_2 core particles, as shown in Fig. 5. For individual pure particles of SiO_2 and ZrO_2, the surface charge originating from unbound sites on the surface was positive at a low pH and became negative at a pH beyond the iso-electric point (IEP). It is already known that the IEP of ZrO_2 particles (IEP = 5.3) is higher than that of SiO_2 particles (IEP = 2.4) due to the stronger electro-attraction of zirconium compared to that of silicon. Thus, in the case of the core–shell particles, it was interesting to find that the behavior of the surface charge and IEP according to the pH was very similar to that of ZrO_2 particles, implying that the core particles of SiO_2 were completely shelled with ZrO_2.

The formation of a chemical bond at the interface of the core–shell particles by the sol–gel process was examined using FT-IR. As shown in Fig. 6, the SiO_2 particles typically showed an asymmetric stretching vibration peak of Si–O–Si at around 1100 cm^{-1}. However, the core–shell particles showed a shift in the characteristic band of asymmetric stretching vibration at 1100 cm^{-1} to lower wave number. According to Zhan and Zeng [11] and Lee and Condrate [12], this shift in the 1100 cm^{-1} band is due to the strong electro-positivity of zirconium in a Si–O–Zr bond, and the degree of the band-shift depends on the number of Si–O–Zr bonds. Therefore, in the present study, this confirmed a chemical bond of Si–O–Zr at the interface between the core and the shell, probably formed by the condensation of zirconium hydroxide with silane groups of isolated silanol, germinals, and vicinals on the surface of the SiO_2 core particles during the sol–gel process. According to Kong et al. [13], silane groups on SiO_2 particles were originated from the incomplete condensation of TEOS. Thereby, in the present study, existence of the silanol groups on the SiO_2 core particles was confirmed by characteristic peaks of vibration bands of Si–OH at 470 and 803 cm^{-1} from the ring structure of Si–O bonds [14,15] and the amount of silanol groups was measured as approximately 25 OH/nm^2 by using TGA [13]. However, when the core particles were coated with ZrO_2 shell, it resulted in a gradual reduction of peak intensity of vibration bands of Si–OH, because the formation of Si–O–Zr bonds decreased the concentration of silane groups on the surface of the SiO_2 core particles.

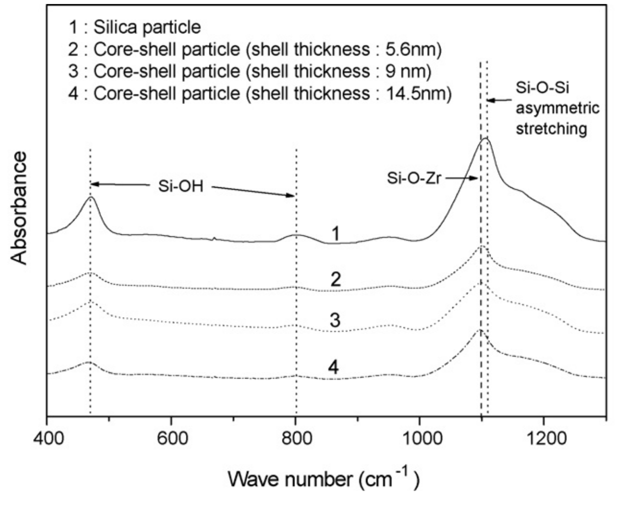

Fig. 6. FT-IR spectra for SiO_2 and core–shell particles with various ZrO_2 shell thicknesses.

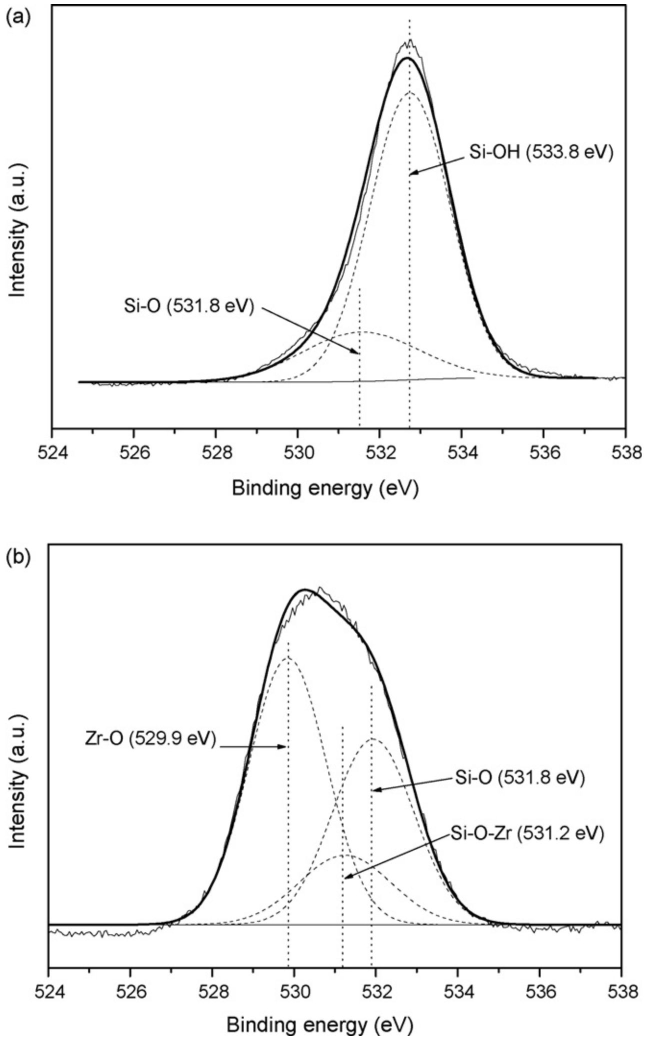

Fig. 7. O 1s XPS spectra for (a) SiO_2 particles and (b) core–shell particles.

The XPS spectra confirmed the formation of Si–O–Zr bonds, as shown in Fig. 7. Plus, the O1s spectra of the SiO_2 core particles revealed two oxygen band peaks for Si–O and Si–OH at 531.8 eV and 533.8 eV, respectively (Fig. 7(a)), as previously reported by Viard et al. [16]. Meanwhile, three oxygen band peaks were observed for the core–shell particles (Fig. 7(b)), where the two peaks at 531.8 and 529.9 eV were from the Si–O and Zr–O bonds of the core and shell, respectively [17], while the third peak at 531.2 eV was due to the shift of Si–O–Zr, as the O1s core electron binding energy was reduced as Si–O was bonded with Zr at the interface of the core–shell particles. Therefore, the results implied the involvement of both chemical and physical bindings between SiO_2 and ZrO_2 in the formation of the ZrO_2 shell around the SiO_2 core particles.

4. Conclusions

Uniform core–shell particles of SiO_2 core-coated with ZrO_2 were prepared using a sol–gel process. The nano-primary particles of ZrO_2 generated by the sol–gel process were shown to be deposited on the SiO_2 core particles to form a shell. The shell thickness and uniformity of the core–shell particles were also found to be strongly dependent on the reaction conditions, including the TBOZ and H_2O concentrations and temperature. Thus, the shell thickness monotonically increased up to 15 nm when promoting the generation of ZrO_2 by increasing the reaction conditions. However, beyond a certain level of reaction conditions, the over enhanced generation of ZrO_2 resulted in the homo-nucleation of stable ZrO_2 particles and aggregation of the core particles.

The zeta-potential measurements confirmed that the SiO_2 core particles were completely shelled with ZrO_2. In addition, FT-IR and XPS showed that a chemical bond of Si–O–Zr was formed during the deposition of ZrO_2 on the SiO_2 core particles due to the condensation of zirconium hydroxide with silane groups on the core particles.

Acknowledgement

This work supported by the KISTEP New Chemical Process Program under contract number M10322010002-03B30001-00210.

References

[1] C.W. Chen, T. Sarizawa, M. Akashi, Preparation of platinum colloids on polystyrene nanospheres and their catalytic properties in hydrogenation, Chemistry of Materials 11 (1999) 1381–1389.

[2] M. Bruchez, M. Moronne, P. Gin, S. Weiss, A.P. Alivisatos, Semiconductor nanocrystals as fluorescent biological labels, Science 281 (1998) 2013–2016.

[3] E. Matijevic, Uniform inorganic colloid dispersions. Achievements and challenges, Langmuir 10 (1994) 8–16.

[4] F. Caruso, Nanoengineering of particle surfaces, Advanced Materials 13 (2001) 11–22.

[5] M. Ocaña, M. Andrès-Vergès, R. Pozas, C.J. Serna, Spherical iron/silica nano composites from core–shell particles, Journal of Colloid and Interface Science 294 (2006) 355–361.

[6] A.B.R. Mayer, W. Grebner, R. Wannemacher, Preparation of silver-latex composites, The Journal of Physical Chemistry B 104 (2000) 7278–7285.

[7] F. Garbassi, L. Balducci, R. Ungarelli, Sol–gel preparation and characterization of spherical ZrO_2–SiO_2 particles, Journal of Non-Crystalline Solids 223 (1998) 190–199.

[8] Z.G. Shi, Y.Q. Feng, L. Xu, M. Zhang, S.L. Da, Preparation and evaluation of zirconia-coated silica monolith for capillary electrochromatography, Talanta 63 (2004) 593–598.

[9] K.S. Kim, J.K. Kim, W.S. Kim, Influence of reaction conditions on sol-precipitation process producing silicon oxide particles, Ceramics International 28 (2002) 187–194.

[10] R.K. Iler, The Chemistry of Silica, John Wiley & Sons, Inc., Canada, 1979

[11] Z. Zhan, H.G. Zeng, A catalyst-free approach for sol–gel synthesis of highly mixed ZrO_2–SiO_2 oxides, Journal of Non-Crystalline Solids 243 (1999) 26–38.

[12] S.W. Lee, R.A. Condrate, The infrared and Raman spectra of ZrO_2-SiO_2 glasses prepared by a sol–gel process, Journal of Materials Science 23 (1988) 2951–2959.

[13] J.M. Kim, S.M. Chang, S.M. Kong, K.S. Kim, J.S. Kim, W.S. Kim, Control of hydroxyl group content in silica particle synthesized by the sol-precipitation process, Ceramics International, (2008) in press.

[14] K. Kamiya, T. Yoko, K. Tanaka, T. Takeuchi, Thermal evolution of gels derived from $CH_3Si(OC_2H_5)_3$ by the sol–gel method, Journal of Non-Crystalline Solids 121 (1990) 182–187.

[15] A. Fontana, E. Moser, F. Rossi, R. Campostrini, G. Carturan, Structure and dynamics of hydrogenated silica xerogel by Raman and Brillouin scattering, Journal of Non-Crystalline Solids 212 (1997) 292–298.

[16] J. Viard, E. Beche, D. Perarnau, R. Berjoan, J. Durand, XPS and FTIR study of silicon oxynitride thin films, Journal of the European Ceramic Society 17 (1997) 2025–2028.

[17] H.J.M. Bosman, A.P. Pijpers, A.W.M.A. Jaspers, An X-ray photoelectron spectroscopy study of the acidity of SiO_2–ZrO_2 mixed oxides, Journal of Catalysis 161 (1996) 551–559.